

The Impact of Quantization on the Design of Solar Power Systems for Cellular Base Stations

*Original*

The Impact of Quantization on the Design of Solar Power Systems for Cellular Base Stations / Ana Paula Couto Da, Silva; Renga, Daniela; Meo, Michela; AJMONE MARSAN, Marco Giuseppe. - In: IEEE TRANSACTIONS ON GREEN COMMUNICATIONS AND NETWORKING. - ISSN 2473-2400. - ELETTRONICO. - 2:1(2018), pp. 260-274. [10.1109/TGCN.2017.2762402]

*Availability:*

This version is available at: 11583/2685067 since: 2022-03-26T12:46:03Z

*Publisher:*

IEEE

*Published*

DOI:10.1109/TGCN.2017.2762402

*Terms of use:*

This article is made available under terms and conditions as specified in the corresponding bibliographic description in the repository

*Publisher copyright*

IEEE postprint/Author's Accepted Manuscript

©2018 IEEE. Personal use of this material is permitted. Permission from IEEE must be obtained for all other uses, in any current or future media, including reprinting/republishing this material for advertising or promotional purposes, creating new collecting works, for resale or lists, or reuse of any copyrighted component of this work in other works.

(Article begins on next page)

# The Impact of Quantization on the Design of Solar Power Systems for Cellular Base Stations

Ana Paula Couto da Silva, Daniela Renga, Michela Meo and Marco Ajmone Marsan

**Abstract**—In this paper we focus on the design of the power system for off-grid cellular base stations powered by a photovoltaic (PV) solar panel and a battery. Several papers already tackled this problem, with different approaches, modeling either the day-to-day behavior, or the hourly dynamics. In addition, the meteorological characteristics were modeled using a variable number of levels. Different approaches produced different results, hardly comparable. In this paper, we discuss the choice of parameter quantization for time, weather, and energy storage, with the objective of deriving guidelines for the development of accurate and credible models that can support the power system design. Our investigation shows that quantization has an important impact on the mathematical model outputs. Hence, quantization must be carefully taken into account, to achieve a correct dimensioning of the power system.

**Index Terms**—Base stations, Renewable energy sources, Markov processes.

## I. INTRODUCTION

**A**FTER more than a decade of intense research in the field of green (or energy-efficient) communications and networking, we can draw some conclusions and observe a number of effects. First of all, the attitude towards energy issues of network operators in general, and of mobile network operators (MNOs) in particular, has drastically changed. Now, energy is viewed as an important portion of the network operational expenditures (OPEX), and parsimonious approaches are considered extremely important [1]. Second, the design of the new generations of network equipment (base stations - BSs - in particular, in the case of mobile networks) has included among the key performance indicators also energy consumption; this has brought peak power consumption down from the usual 3.5 kW of a 2G macro BS to around 750 W for new LTE macro BSs [2], and much less for micro BSs and small cell BSs. Third, the vast body of research work in network management algorithms [3], mostly proposing the consolidation of network capacity in only few active elements in periods of low traffic, the other elements being placed in sleep modes, has not yet had a significant impact on the way networks are managed, primarily because operators fear coverage holes, or glitches in the network performance under unexpected traffic conditions, or increased failure rates due to frequent switchoff/switchon.

Ana Paula Couto da Silva is with the Computer Science Department, Universidade Federal de Minas Gerais, Brazil.

Daniela Renga and Michela Meo are with the Electronics and Telecommunications Department, Politecnico di Torino, Italy.

Marco Ajmone Marsan is with the Electronics and Telecommunications Department, Politecnico di Torino, Italy, and IMDEA Networks Institute, Leganes, Spain.

Manuscript received xx/xx/2017; revised xx/xx/2017.

A very important consequence of the much improved energy efficiency of new BS generations is that renewable energy sources (RES) have become a viable option to power cellular networks [4]. This is particularly relevant when we consider the need to bring cellular network services to portions of the world population that do not have access to a reliable power grid.

Indeed, after a first wave of diffusion of cellular networks in the western world, and a second wave in the far east, the third wave of diffusion of cellular networks and services (the next billion users) is expected to be in Africa, and in West Africa countries in particular [5]. However, in very populated countries of West Africa (like Nigeria, the 7th most populated country of the world), only a limited percentage of the population has access to the power grid (55% in Nigeria), with frequent and long power cuts. In this context, powering the BSs that are necessary to establish a cellular telecommunication service is a problem. The solution most frequently adopted by operators relies on Diesel power generators, which are however extremely costly, because of the price of fuel, the need to transport fuel and to schedule frequent preventive maintenance in remote locations, and because of fuel thefts. Under these circumstances, considering also the climate of the West Africa region, and the increased power efficiency of equipment, the use of RES, and of solar power in particular, has become an extremely attractive option, which is adopted in a growing number of cases [6].

The solar solution for powering BSs is not only interesting in regions where the power grid is not available or not reliable. It can be economically effective also in rural areas, where the cost of bringing a power cable to the BS may be higher than that of a solar panel. Even in urban environments, bringing a power connection to a BS may require digging across a street or a park, with the associated bureaucracy burden.

Furthermore, the ICT sector accounts for around 2% of the global carbon emissions [7]. In particular, telecom operator networks consume 254 TWh per year, making up 77% of the total worldwide electricity consumption in communication networks, with an annual growth rate higher than 10% [8]. The contribution of mobile networks alone to the global carbon footprint was already 0.2% back in 2012 (comparable with the worldwide carbon emissions of airplanes), and their impact on carbon emissions is bound to further increase in the next years [7]. Hence, the use of renewable energy sources to power BSs can also help in greatly reducing the carbon footprint of cellular networks, with obvious benefits for the environment.

For these reasons, several papers have already been looking at the possibility of powering BSs with solar energy, consid-

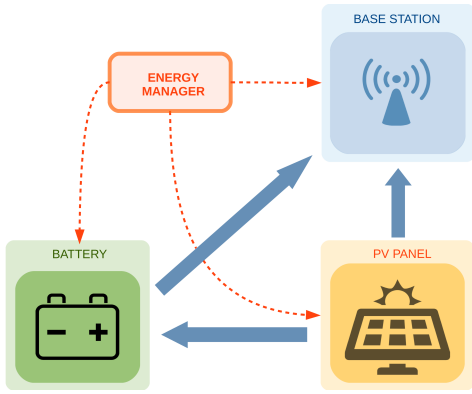


Fig. 1. BS powered by a PV panel and equipped with an energy storage system. The energy flows are represented by the bold blue arrows, whereas the dashed red arrows refer to the energy management.

ering a setup where the BS is paired with a photovoltaic (PV) solar panel, and a battery for energy storage, so that the BS can operate also when the PV panel is not producing energy [9], [10], [11], [12], [13]. More precisely, the system that is normally studied, and that we also consider in this paper, is as shown in Figure 1. It comprises a BS, which is the power consumer, a PV panel, which is the power producer, a battery, or a set of batteries, which form the energy storage unit, and an energy manager. The energy manager sends the power produced by the PV to the BS, and any excess power to the battery. At the same time, if the power produced by the PV panel is less than required by the BS, the energy manager extracts power from the battery, as long as energy is available. Of course, it may happen that some of the power produced by the PV panel is lost, because the battery is full. It can also happen that the BS must be turned off, because the PV panel is not producing enough power, and the battery is empty. Both of these events are undesirable. The former because it leads to energy waste, the latter because it leads to service interruption. A careful design of the system must minimize the impact of these events.

The system of Figure 1 is simplified with respect to what exists in many BS sites. Indeed, very frequently the PV panel output is transformed from DC to AC by an inverter. Some of the AC power is used to run the hardware cooling system, and the site lights. The rest of the AC power is converted to DC again to power the BS equipment. Some of the newest BS equipment run with little or no cooling, and can accept direct DC input. This can save the double conversion DC-AC-DC with the associated losses. In addition, a number of solar-powered BS sites also include an auxiliary power source, which often is a Diesel generator.

The dimensioning of the BS solar power system can be tackled by exploiting probabilistic models which consider the amount of energy produced by a solar panel, the amount of energy consumed by the BS, and the capacity of the energy storage. While the real problem is continuous both in time and in the (random) amounts of energy produced and consumed, the models that appeared so far in the technical literature look at the quantized version of the problem, for mathematical

tractability. This means that a time slot is defined, to account for energy production and consumption, and that the amount of energy stored in the battery is also discretized. Even the weather characteristics, in terms of the solar irradiance, which obviously define the amount of produced energy, are normally quantized, so as to simplify the probabilistic model.

This paper looks at the effect of these quantizations, and provides answers to the following questions: i) how to quantize the weather characteristics? ii) what is a reasonable time slot duration? iii) how finely should the battery capacity be quantized? These questions arise from the consideration that in previous works, as we see in the next section, very different approaches were used for quantization: time slots vary between 1 day and 1 hour, stored energy quanta vary between 100 Wh and 20 kWh, solar irradiance levels vary from 3 to 10. Authors never discuss the reasons for their choices.

Our key contribution is to provide a clear understanding of the effects of quantization, and to allow the selection of the best values for the model parameters. The general conclusions that come out of our investigation are that it is reasonable to classify the daily solar irradiance in a number of levels around 5, provided that the quantization of the weather characteristics is carefully implemented, that the time slot granularity should be around 60 minutes, and that characterizing the filling of the battery capacity with a quantum corresponding to roughly 10% of the energy consumed in a time slot is sufficient.

The rest of this paper is organized as follows. In Section 2 we overview the previous research in this field. In Section 3 we introduce the system model, and in Section 4 we discuss the issue of quantization. Section 5 presents and discusses some numerical results. Finally, Section 6 concludes the paper.

## II. RELATED WORK

The increasing relevance of renewable energy sources in powering mobile communication networks motivated several research groups to investigate the topic, so that a number of papers have already appeared in the technical literature. Some works focus on exhaustive overviews of sustainable and green mobile networks deployment worldwide [14], [15], [16], [17]. Other works, instead, aim at modeling the behavior of BS power systems based on renewables, with the objective of understanding the characteristics of these systems, so as to provide guidelines for correct dimensioning [9], [10], [11], [12], [13], [18], [19].

Most related with this paper are the works in [13], [18], [19], where the authors relied on Markovian models for computing the BS outage probability when cellular BSs are powered by solar energy. [13] proposes a discrete-time Markov chain of the battery charge at the BS. As stated by the authors, the model can be used to quantify the relationship between system parameters, such as PV panel size, battery size, harvested solar energy and load profiles, on the BS outage probability. In this model, time is discretized with time slots of 1 hour. As regards weather conditions, each day is classified according to 3 categories, resulting in 3 different possible levels of daily renewable energy production, and of harvested energy profiles. The battery charge level is quantized into rather large blocks

of 1 kWh. In [18], a Markov-chain-based energy storage model is defined, to develop a power availability framework for PV panel generation. The model may assist in planning both large and small-scale grid-integrated PV generation, and also quantify power availability. This work investigates the application of the model in a scenario where the load is represented by 300 households, with an average daily energy usage of about 17.6 kWh per household. The time granularity adopted in this study is 1 hour, whereas the energy storage is quantized into steps of 20 kWh (note that the average hourly energy consumption is about 220 kWh, so that the battery charge quantization is about 1/10 of the energy consumption in a time slot). No classification of the daily level of renewable energy production based on historical data is considered.

Leonardi *et al* [19] consider two Markov chain models in their analysis: the first one based on solar irradiation data in two consecutive days, and the second based on solar irradiation data in triples of consecutive days, with the objective of exposing the influence of correlations in weather conditions. Different numbers of quantization levels (5, 8 and 10) are considered for the daily irradiance. A fixed number of quantization levels is assumed for the energy storage, equal to 100, hence the discretization step sizes vary depending on the considered battery capacity (10 kWh, 25 kWh, 50 kWh). Both solar energy generation and energy consumption are accounted on a daily basis. Moreover, only the impact of different battery size on the system performance is analyzed. The main result is that both models produce almost equivalent results, so that the impact of weather correlation is small.

Although our model is similar to the one based on solar irradiation data in two consecutive days proposed in [19], to the best of our knowledge, this is the first work that carefully investigates the impact of quantization of i) weather characteristics, ii) time slot duration, and iii) battery capacity, on the key performance measures of power systems based on renewable energy for cellular network BSs. Our results show that the discretization steps play a significant role in understanding the behavior of such power systems, hence in correctly dimensioning them.

### III. THE SYSTEM MODEL

A probabilistic model of the system must account for the energy production process, for the energy consumption process, and for the evolution of the battery charge with time. In particular, the model must account for the periods of the day in which energy production is significant (how high depends on the weather conditions), and for the periods of no production, for example at night. The model must also consider that the BS power consumption varies during the day according to the volume of services offered to end users.

In this section, we first present the probabilistic model of the system behavior. Next, we introduce the energy consumption model used in our analysis in Section III-B. Transitions probabilities are defined in Section III-C. Finally, the key performance indicators for the BS solar power system are described in Section III-D.

#### A. Model Formulation

We define a discrete time Markov chain (DTMC) model over time slots of duration  $\Delta T$  [h]. The DTMC state is defined by three variables:

$$\bar{s} = (W, T, S)$$

where  $W$  indicates the weather state;  $T$  represents the time of the day, and  $S$  corresponds to the current charge of the battery.

The time granularity  $\Delta T$  drives the dynamics of the DTMC model. The daily evolution of the system spans a number of time slots equal to  $N_T = 24/\Delta T$ . Hence, the DTMC moves from a state with  $T = i, i \in \{0, 1, \dots, N_T - 1\}$  to a state with  $T = (i + 1 \bmod N_T)$ .

The value of the weather variable  $W$ , together with the PV panel size, and energy loss parameters, determines the amount of energy produced by the PV panel in a time slot.  $W$  defines if a day is sunny (high production) or cloudy (low production). Then, the production in a given time slot depends on both  $W$  and the time of the day represented by the time slot: for example, whatever the value of  $W$  is, time slots that correspond to night hours have zero production, while time slots that correspond to midday have large production levels, whose actual value depends on  $W$ , i.e., on whether the day is sunny or cloudy. Since  $W$  defines the weather in a day, its value changes only at the beginning of a new day, that is with the transition of the variable  $T$  from the value  $N_T - 1$  to the value 0.

The definition of possible values for  $W$  is based on long-term (20 years) historical data about the daily solar irradiance. The daily solar irradiance is quantized over a number of levels equal to  $N_W$ , so that we can define  $N_W$  types of daily weather,  $W_i$ , with  $i \in \{1, N_W\}$ . From the same data we compute the probability that after a day of type  $W_i$  a day of type  $W_j$  follows, with  $i, j \in \{1, N_W\}$ . Given a daily solar irradiance level  $W_i$ , the irradiance over time slots is derived from fine-grained short-term (2 years) solar irradiance historical data, that reflect the variability of irradiance in different moments of the day, with low irradiance occurring after dawn and before sunset, and peaks occurring around midday. From the historical data (long- and short-term), for each type of day, and for each time slot, we compute the average energy production. The data about solar irradiance are taken from the SoDa service<sup>1</sup>.

Finally, the state variable  $S$  represents the battery charge level. Let  $C_B$ , measured in kWh, represent the battery capacity. By choosing a quantization step  $Q_s$ , the set of values for  $S$  is  $\{0, 1, \dots, N_S\}$ , with  $N_S = C_B/Q_s$ .

At every DTMC state transition, we compute the energy level in the battery at the beginning of the next slot as the sum of the energy already in the battery at the beginning of the current slot, plus the energy produced during the time slot (that depends on  $W$  and  $T$ ), minus the energy consumed in the same time slot (that depends on  $T$ ). The value of  $S$  is the

<sup>1</sup><http://www.soda-pro.com/>. Two different data sets are used: the first one provides solar irradiance data at 15 minutes intervals for a period of 2 years, with a spatial resolution of about 5 km; the second one provides daily solar irradiance data for a period of 20 years, with a spatial resolution of about 20 km

TABLE I  
PARAMETERS OF THE POWER CONSUMPTION MODEL FOR A LTE MACRO BS [21].

Macro BS Type	$N_{TX}$	$P_{max}[W]$	$P_0[W]$	$\Delta_p$
With RRU	6	20	84	2.8

energy in the battery at the beginning of the time slot, while the energies produced and consumed refer to the whole time slot (they are the integrals of the respective powers during the time slot).

### B. Energy Consumption Model

The European project EARTH developed a model [20] to estimate the power consumption of a macro BS, which has become the standard in the field. The power needed to operate a macro BS can be expressed as:

$$P_{in} = N_{TX} \cdot (P_0 + \Delta_p \cdot P_{out}), \quad 0 < P_{out} < P_{max} \quad (1)$$

where  $N_{TX}$  is the number of BS transceivers,  $P_{max}$  represents the maximum radio frequency output power at full load for one transceiver,  $P_0$  corresponds to the fixed power consumption for one transceiver when the radio frequency output power is null, and  $\Delta_p$  is the slope of the load-dependent power consumption. Typical values of the parameters are listed in Table I for a LTE macro BS with Remote Radio Unit (RRU).

$P_{out}$  is derived as:

$$P_{out} = \rho \cdot P_{max}, \quad 0 \leq \rho \leq 1 \quad (2)$$

where  $\rho$  denotes the instantaneous normalized BS load.

In order to characterize the parameter  $\rho$ , and its variability during the day, we consider the traffic profiles corresponding to real traces provided by one of the Italian mobile network operators [21]. The daily traffic profiles for a cell in a business area (BA) and a cell in a residential area (RA), during week-day (wd) and week-end (we), measured in a network in operation are provided in Figure 2. Traffic values are obtained by averaging and normalizing the measurements collected at 15-minute intervals during a week. Normalization is such that, for both BA and RA, the maximum 15-minute average load is set equal to the maximum load that can be carried by the BS (i.e.,  $\rho = 1$ ). This is quite a pessimistic assumption in terms of power consumption, since significant levels of overprovisioning exist in the network, especially when a new high-capacity technology is introduced (as is now happening with 4G), but guarantees that the performance targets are met for any BS load. For both the business and residential profiles, traffic fluctuates significantly during a day, and periods of low activity are long. Figure 3 shows the corresponding energy consumption, computed with the EARTH model above for a macro cell with RRU. In the BA cell, the typical week-day traffic load is very low at night, then traffic starts increasing around 8am. Load peaks occur in the central hours of the day, decreasing again after 5pm. In the week-end, traffic remains low for the whole day. We observe, however, that, even during low traffic load periods, around 500 W are consumed by the macro BS due to cooling, signalling, baseband processing, etc

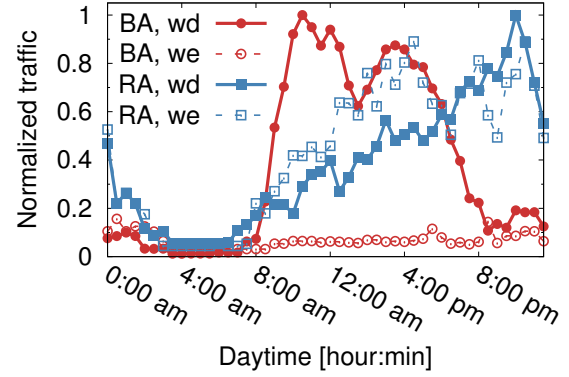


Fig. 2. Week-day (wd) and week-end (we) traffic loads in a business (BA) and residential (RA) area.

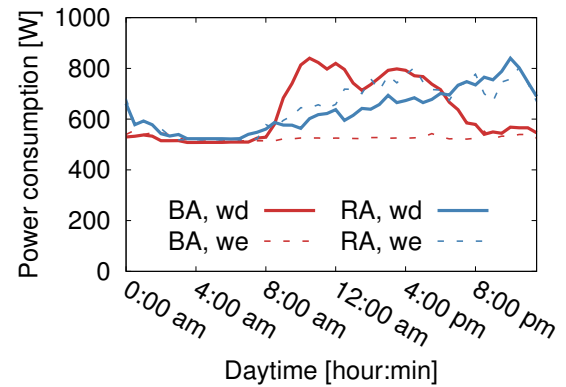


Fig. 3. Week-day (wd) and week-end (we) energy consumption for an LTE macro BS with RRU in a business (BA) and residential (RA) area, based on the EARTH model [20].

[22]. In the case of the RA cell, a more gradual increase in the traffic load is observed from morning to night, and differences between week-day and week-end are marginal. Similar to the BA profile, power consumption never goes below half a kW.

### C. Transition Probabilities

The DTMC model deployed to investigate the renewable powered mobile system operation is depicted in Figure 4, where only some of the state transitions are shown. Each state  $\bar{s}_i = (W_i, T_i, S_i)$  is characterized by different values of day-type  $W_i$ , time of the day  $T_i$  and battery charge level  $S_i$ . Only a sample of all the possible transitions between different states is highlighted in the figure. In particular, the transitions starting from states  $(W_i, 0, S_i)$  and  $(W_i, N_T - 1, S_i)$  are represented. These states correspond to the first and last timeslots of a day of each type  $W_i$ , respectively, with any possible value of battery charge level. The cardinality of the state space of the DTMC model is the product of the number of time slots during a day  $N_T$ , times the number of solar irradiance levels  $N_W$ , times the number of levels considered for the battery charge  $N_S + 1$ .

However, since the type of day can change only when a new day starts, given the type of day and the daily traffic profile, the transition from a state  $\bar{s}_i$  to a state  $\bar{s}_j$ , with  $\bar{s}_i = (W_i, T_i, S_i)$ , and  $\bar{s}_j = (W_j, T_j, S_j)$ , with  $T_i \in \{0, 1, \dots, N_T - 2\}$ , is possible

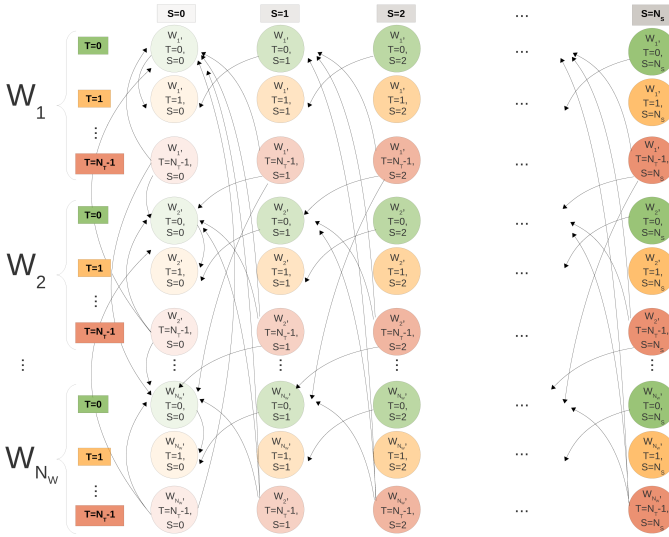


Fig. 4. Markovian model representing the renewable powered mobile system operation.

only with  $W_j = W_i$  (the type of day cannot change during the same day),  $T_j = T_i + 1$  (the time slot increases along the same day), and  $S_j - S_i$  equal to the (fixed) difference between the energy produced and consumed during the time slot.

On the contrary, the transition from a state  $\bar{s}_i$  to a state  $\bar{s}_j$ , with  $T_i = N_T - 1$  is possible with any value of  $W_j$  (the type of day can change at the beginning of a new day),  $T_j = 0$  (the first time slot of the new day), and  $S_j - S_i$  equal to the energy consumed during the time slot (no solar irradiation is present around midnight at the considered latitudes).

As it can be observed from Figure 4, this means that for all states  $\bar{s}_i$  with  $T_i = N_T - 1$  the number of possible outgoing transitions is equal to the number of day-types  $N_W$ , while for all other states only one outgoing transition is possible. As a result, the DTMC transition probability matrix is quite sparse.

#### D. Performance Measures

From the steady-state solution of our DTMC model, we evaluate a few key performance indicators for the BS power system. Let  $\pi(\bar{s}) = \pi(W, T, S)$  be the steady-state probability of state  $\bar{s} = (W, T, S)$ , with  $W \in \{0, \dots, N_W - 1\}$ ,  $T \in \{0, \dots, N_T - 1\}$ ,  $S \in \{0, \dots, N_S\}$ .

We define:

- 1)  $E[S]$ , the average battery level:

$$E[S] = \sum_{\forall W} \sum_{\forall T} \sum_{\forall S} S \pi(W, T, S);$$

- 2)  $P_e$ , the empty battery probability:

$$P_e = \sum_{\forall W} \sum_{\forall T} \pi(W, T, 0);$$

- 3)  $P_f$ , the full battery probability:

$$P_f = \sum_{\forall W} \sum_{\forall T} \pi(W, T, N_S).$$

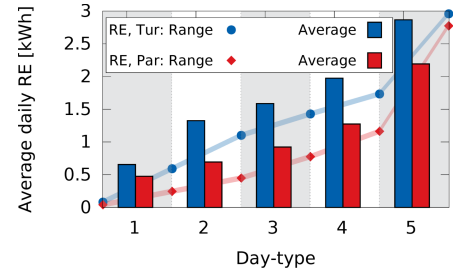


Fig. 6. Day-type average values of daily renewable energy (RE) production of a 1 kW peak PV panel, for 5 day-types ( $N_W=5$ ) with equal-probability discretization, in Turin and Paris, along with the corresponding discretization levels of daily RE.

#### IV. MODEL PARAMETRIZATION

We now discuss the main model design choices, as regards the effect of the discretization of the energy production and consumption models (Section IV-A), discretization of time (Section IV-B), and of energy storage (Section IV-C). Then, we present some lessons learned from our analyses (Section IV-D).

##### A. Energy Production Model

As previously mentioned, the parameters of the energy production stochastic model are derived from traces available in the Solar Radiation Data (SoDa) website. In particular, we used the SoDa 20-year trace collected from January 1st 1985 to December 31st 2004 in the cities of Turin, Italy, Paris, France, and Maiduguri, Nigeria. This data is provided by NASA (USA) and MINES Paris Tech/Armines (France), considering global radiation in the horizontal plane. In the cases of Turin and Paris, for each year we only looked at the 3 winter months (December, January, February, i.e., 90 or 91 days per year). These are the periods which result most critical for the solar power system design, because of shorter daylight periods and lower irradiance levels at the latitudes of Turin and Paris, in the winter season of the northern hemisphere. As shown in [19], if the solar power system in Turin is dimensioned based on the summer period, its performance in winter becomes unacceptable. We will instead consider the 3 most rainy months (July, August and September) when looking at the Maiduguri location in Section V.

Starting from the individual values of the daily energy production of a 1 kW peak solar panel (i.e., a solar panel large enough to produce an output power of 1 kW in standard conditions, including a solar irradiance of 1 kW/m<sup>2</sup> – about 5 m<sup>2</sup> with the current normal solar cells), we first created a histogram by applying an equal-range discretization. That is, we first divided the total production range (i.e., the difference between the maximum and minimum productions observed over the 20-year period) into  $N_W$  ranges of equal size. Then, we computed the frequency (probability) of each interval, and defined  $N_W$  energy production levels as the middle values of each interval. Figure 5 reports the histograms, and the daily energy production ranges, in the two cases  $N_W = 5$  and  $N_W = 10$ . The blue bars in the histograms refer to Turin, while the red ones refer to Paris. Probabilities are reported



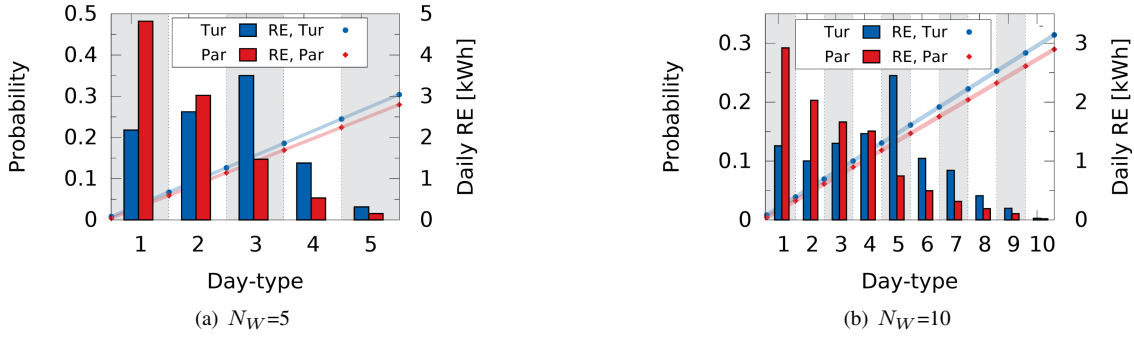


Fig. 5. Day-type probability distribution for 5 and 10 day-types ( $N_W=5$  and  $N_W=10$ ) with equal-range discretization, in Turin and Paris, with corresponding daily produced renewable energy (RE) discretization levels, assuming a 1 kW peak PV panel.

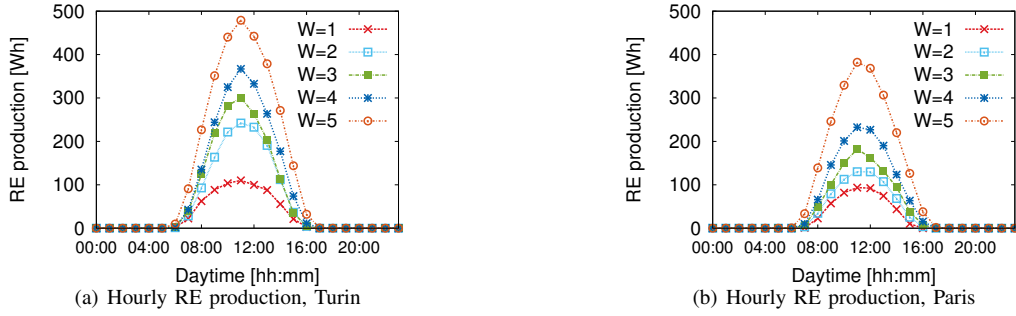


Fig. 7. Hourly energy production of a 1 kW peak PV panel, per each day-type in Turin and Paris, for  $N_W=5$  with equal-probability discretization.

on the left vertical scale. The blue markers are associated with the right vertical scale, and report the extremes of the daily energy production ranges for Turin. The red markers refer instead to Paris. We see, for example, that in the case  $N_W = 10$ , the production range number 5, in the case of Turin has extremes 1.3 kWh and 1.6 kWh, and probability 0.25. The same production range 5 in the case of Paris has extremes 1.2 kWh and 1.4 kWh, and probability 0.075.

It is also possible to create a histogram by applying an equal-probability discretization. That is, to divide the total production range into  $N_W$  ranges of different sizes, so that the frequency of each interval is the same, and to define  $N_W$  energy production levels as the middle values of each interval. Figure 6 reports the energy production levels obtained with this procedure, for  $N_W = 5$ , in the cases of Turin and Paris. With this discretization procedure, the resulting average hourly production for each day-type, with  $N_W=5$ , for Turin is reported in Figure 7(a), and for Paris in 7(b). These curves are generated by using both the long- and short-term solar irradiance datasets, as explained before. We also evaluate the statistical frequency of consecutive day-types. For each daily production level  $W_i$  (i.e., for each day-type  $W_i$ ), we count the number of dataset instances where the following day is of type  $W_j$ , and dividing this number by the total number of day pairs we compute the statistical frequency with which day-type  $W_j$  follows day-type  $W_i$ . The statistical frequency is then mapped into the transition probabilities of the Markov chain. For what concerns the DTMC model design, the most critical decision with respect to energy production is the discretization of the

meteorological data, i.e., the selection of the number  $N_W$  of energy production levels (also called day-types).

Figure 8 depicts the three main performance indicators of the macro BS power system for Turin, namely the average battery charge, and the empty and full battery probabilities, versus values of  $N_W$ , chosen in the set  $\{3, 5, 7, 10\}$ . The quantization of the energy production in this case uses equal-ranges over the Turin data, the battery capacity is 25 kWh, and three different PV panel sizes are used: 20, 30 and 40 kW peak. The time slot is 1 h, and the battery charge quantum is 100 Wh. The results show that the number of day-types has a marginal impact on the performance indicators: the average battery charge varies within less than  $\pm 5\%$ , while empty and full probabilities, whose absolute values are quite small, exhibit acceptable variations. Hence, while a higher number of possible day-types could be considered preferable, because it provides a more accurate distinction among production levels, the impact on results is limited.

Moreover, it must be considered that the choice of  $N_W$  should also take into account the fact that with  $N_W$  energy production levels, we need to estimate  $N_W \cdot N_W$  probabilities that after a day of type  $W_i$  a day of type  $W_j$  follows. A small value of  $N_W$  is thus desirable to guarantee not only a smaller size of the DTMC state space, but also a more reliable estimation of the transition probabilities from the available data. Considering the 3 winter months in 20 years, we have 1,805 days; from which we need to estimate  $N_W^2$  probabilities. With  $N_W = 10$  this means about 18 samples to estimate one probability, in case of uniformly distributed probabilities, but actually much less for infrequent cases (such as the sequence

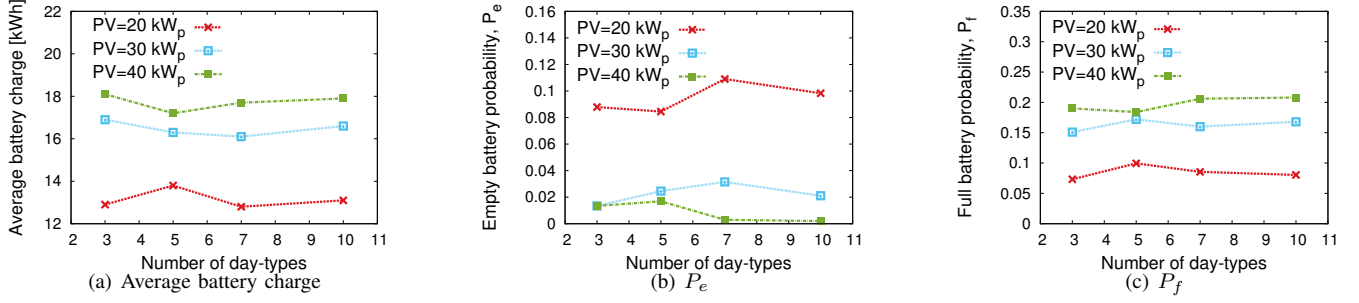


Fig. 8. Average battery charge, empty ( $P_e$ ) and full ( $P_f$ ) battery probabilities versus number of day-types  $N_W$ , for different PV panel sizes, for Turin, with *equal-range discretization* and time slot  $\Delta T = 1$ h, for  $C_B = 25$  kWh,  $Q_S = 100$  Wh, with residential weekday traffic profile, adopting the Earth model.

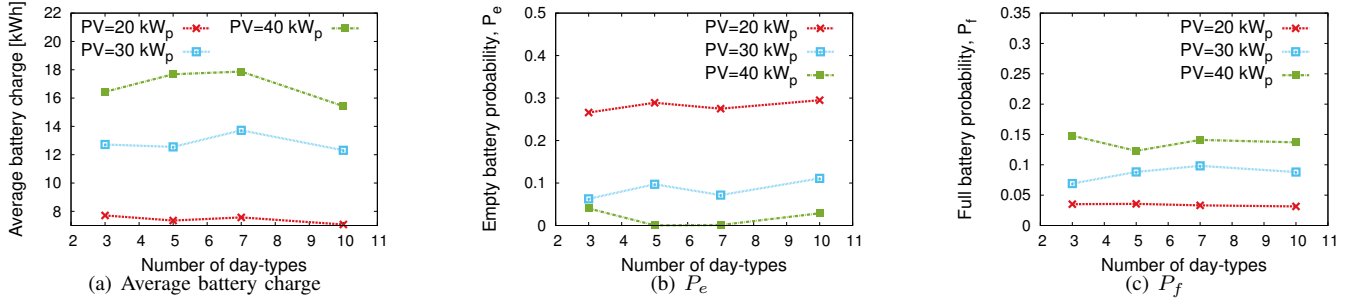


Fig. 9. Average battery charge, empty ( $P_e$ ) and full ( $P_f$ ) battery probabilities versus number of day-types, for different PV panel sizes, for Paris, with *equal-range discretization* and time slot  $\Delta T = 1$ h, for  $C_B = 25$  kWh,  $Q_S = 100$  Wh, with residential weekday traffic profile, adopting the Earth model.

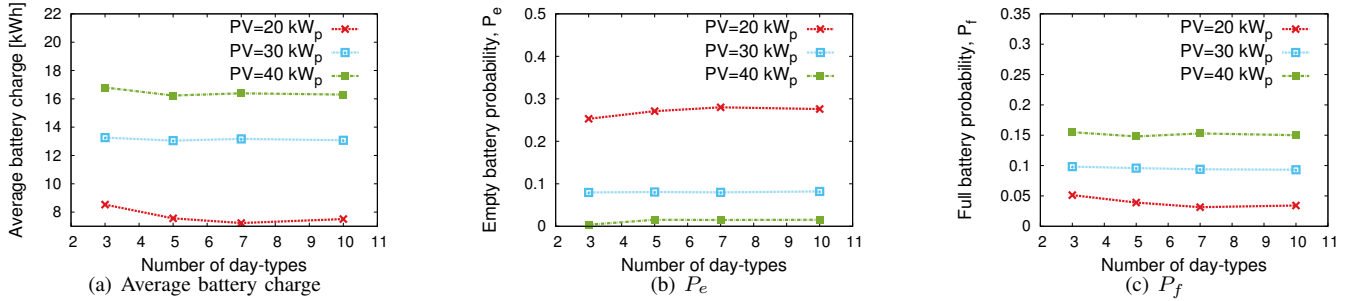


Fig. 10. Average battery charge, empty ( $P_e$ ) and full ( $P_f$ ) battery probabilities versus number of day-types, for different PV panel sizes, for Paris, with *equal-probability discretization* and time slot  $\Delta T = 1$ h, for  $C_B = 25$  kWh,  $Q_S = 100$  Wh, with residential weekday traffic profile, adopting the Earth model.

formed by a very cloudy day followed by a most sunny day). From the results in Figure 8 we can thus conclude that good choices for  $N_W$  could be 5 or 7.

Results for the city of Paris in the same conditions as above are shown in Figure. 9. Paris weather is quite different from the one in Torino, with much quicker variations that are reflected in a somewhat higher variability in the results for different values of  $N_W$ . An explanation for this behavior can be found by looking at the histograms of the daily energy productions in Turin and Paris, shown in Figure 5, for  $N_W=5$  and  $N_W=10$ . The daily energy production histogram in Paris has a triangular shape, so that some energy levels are much more likely to occur than others, meaning that the estimation of transition probabilities for these less likely levels is not accurate. In cases like this one, it can be convenient to adopt an equal-probability (rather than equal-range) discretization. Note that

this is not the case for Turin, whose histogram exhibits rather a bell shape.

The results with this kind of discretization are reported in Figure 10 for the case of Paris, and, as expected, are more stable. The results for the case of Turin are reported in Figure 11, and they show similar stability.

In conclusion, the results of our analysis suggest that, depending on the shape of the day-type histogram, we can choose an equal-range or an equal-probability discretization. When the histogram is bell-shaped either discretization is acceptable. Instead, when the histogram shows a triangular shape, an equal-probability discretization should be preferred. As for the choice of the number of levels  $N_W$ , a trade-off between accuracy in representing the production levels and reliability in the transition probability estimation should be decided.



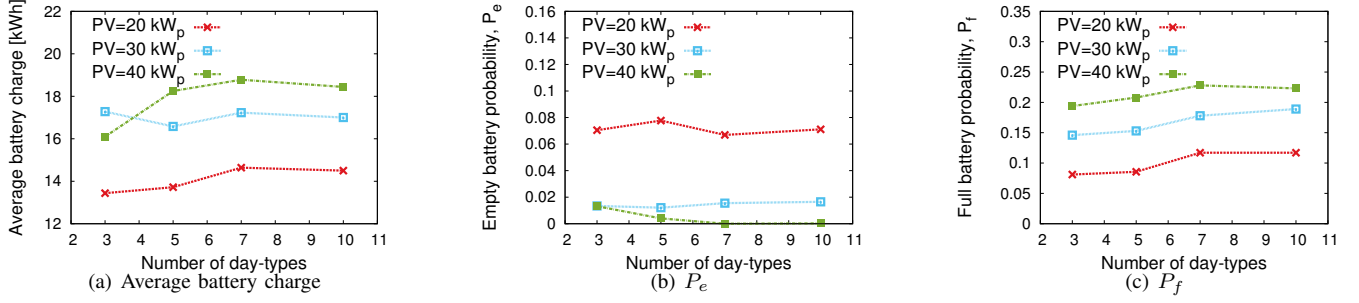


Fig. 11. Average battery charge, empty ( $P_e$ ) and full ( $P_f$ ) battery probabilities versus number of day-types, for different PV panel sizes, for Turin, with equal-probability discretization and time slot  $\Delta T = 1$ h, for  $C_B = 25$  kWh,  $Q_S = 100$  Wh, with residential weekday traffic profile, adopting the Earth model.

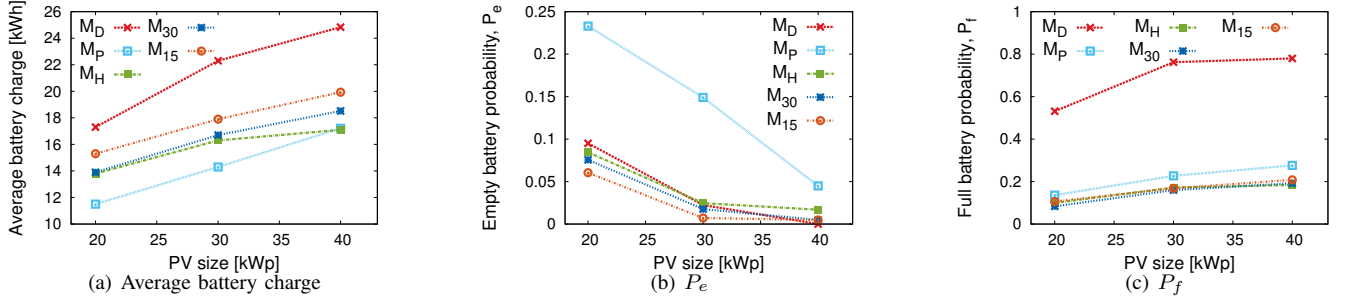


Fig. 12. Average battery charge, empty ( $P_e$ ) and full ( $P_f$ ) battery probabilities versus PV panel size, for different time slots, for Turin, with 5 day-types, with equal-range discretization, for  $C_B = 25$  kWh,  $Q_S = 100$  Wh, with residential weekday traffic profile, adopting the Earth model.

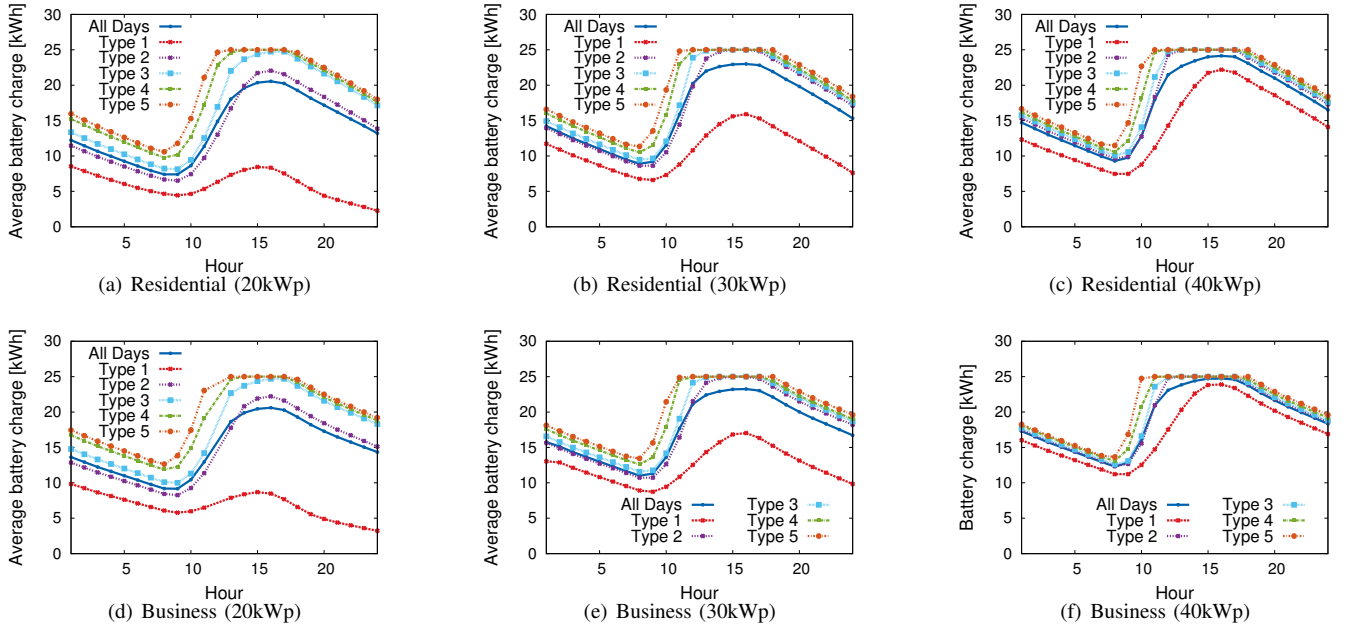


Fig. 13. Average hourly battery charge for a macro BS in Turin versus time, with  $N_W = 5$  and equal-range discretization, time slot  $\Delta T = 1$ h, PV panel sizes 20, 30, and 40 kW peak,  $C_B = 25$  kWh, and  $Q_S = 100$  Wh, for both the residential and business weekday traffic profiles, adopting the Earth model.

### B. Time Granularity

Here, we investigate the impact of the choice of the time granularity, i.e., of the value of the parameter  $\Delta T$ , which represents the time slot in the DTMC model. We consider 5 options: (i) Daily model,  $M_D$  in short, in which  $\Delta T = 24$  h and  $N_T = 1$ ; (ii) Periods of day model,  $M_P$  in short, in

which  $\Delta T = 6$  h and  $N_T = 4$ ; (iii) Hourly model,  $M_H$ , with  $\Delta T = 1$  h and  $N_T = 24$ ; (iv) 30-minute model,  $M_{30}$ , with  $\Delta T = 0.5$  h and  $N_T = 48$ ; and (v) 15-minute model,  $M_{15}$ , with  $\Delta T = 0.25$  h and  $N_T = 96$ . We discuss the effect of time granularity on the data for Turin. Same conclusions hold for the case of Paris.

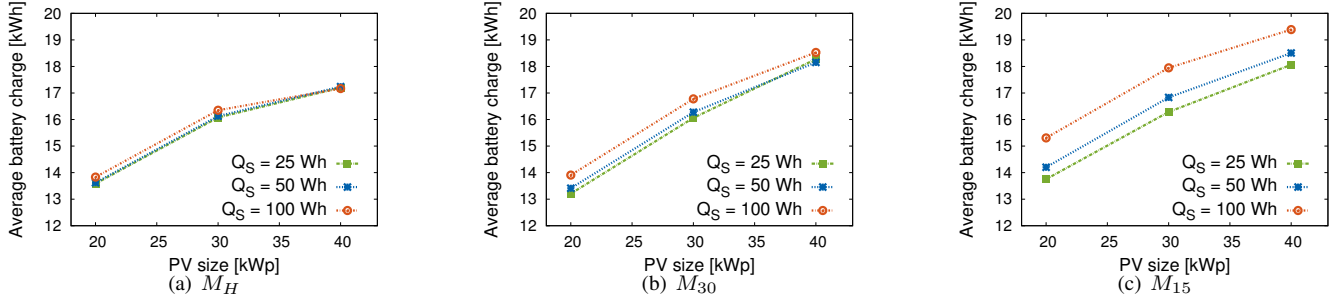


Fig. 14. Average battery charge versus PV panel size, under different discretization values of the energy storage (with capacity  $C_B = 25$  kWh) and for increasing time granularity ( $M_{15}$ ,  $M_{30}$ ,  $M_H$ ), for Turin with  $N_W = 5$  and equal-range discretization, for residential weekday traffic profile, and adopting the Earth model.

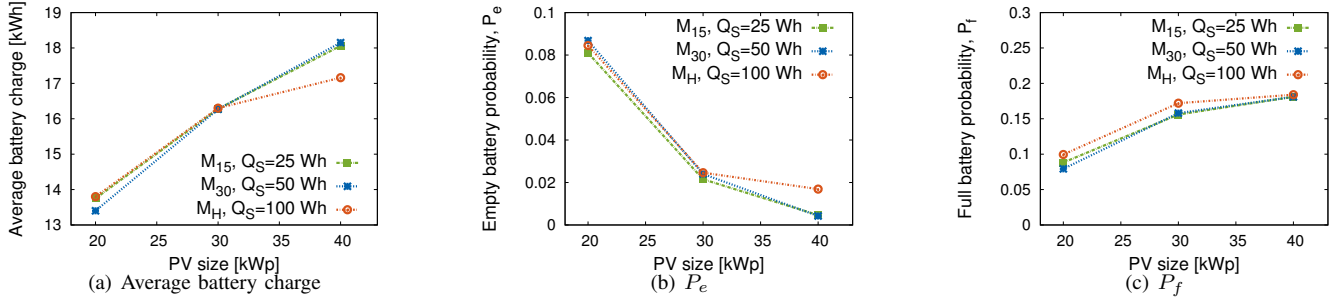


Fig. 15. Average battery charge, empty ( $P_e$ ) and full ( $P_f$ ) battery probabilities versus PV panel sizes, for different time slots, for Turin with  $N_W = 5$  and equal-range discretization, for  $C_B = 25$  kWh, with residential weekday traffic profile, adopting the Earth model.

Figure 12 presents results for a macro BS located in Turin, loaded with the residential traffic profile, and powered by a PV panel of variable size, with energy storage capacity  $C_B = 25$  kWh, modeled with granularity 100 Wh. We can highlight several interesting observations from this first set of results:

- 1) The daily model,  $M_D$ , tends to overestimate the average battery charge and the probability of full battery, when compared against the other considered time granularity models. This is due to the fact that, with this time granularity, the DTMC model globally accounts for all energy produced and consumed in one day, overlooking the short term phenomena, such as, for example, the fact that the battery may become full in some periods during the day, so that the produced energy is lost, even if in other periods of the same day the battery is not full. This phenomenon can be understood by looking at the curves in Figure 13, which show the average battery charge for the case of a macro BS in Turin, with  $N_W = 5$ , PV panel sizes equal to 20, 30, and 40 kW peak, battery capacity equal to 25 kWh, and stored energy granularity equal to 100 Wh, for both the residential and business traffic profiles. The time granularity of the curves is 1 h, and this allows us to see that the daily dynamic of the battery charge is significant. For example, in the top middle plot we see that, in a day of type 5, the battery is full from 11 am to 6 pm. In this period, no energy produced by the PV panel which is not immediately consumed by the macro BS can be stored. For the rest of the day the battery is not full, and the excess energy production can be stored. However, if we look at the whole day, we see

that most of the excess energy production can be stored. This causes the overestimation of the average battery charge, because the highest energy production occurs in the periods when the battery is full.

- 2) The periods of day model,  $M_P$ , with respect to the daily model, tends to better capture the fluctuations between periods of battery charge and discharge during the day, but exhibits a behavior similar to the daily model when the PV panel size grows large, because of the same phenomena mentioned above. Under this model, the empty battery probability results to be significantly overestimated with respect to the other models. This is due to the fact that, besides two 6-hour periods in which the renewable energy production is either null (during night) or very high (in the middle of the day), the other two periods exhibit energy generation profiles that include hours of low production along with hours of higher generation. In these periods, a model with a finer time granularity (e.g. 1 hour) is such that hours with higher production reduce the probability of empty battery (which is measured at the end of the time interval), whereas under the  $M_P$  model the total production over these 6-hour time slots is not enough to balance energy consumption, resulting in a null battery charge at the end of the period.
- 3) The hourly, 30-minute, and 15-minute models generate similar values for the analysed performance measures in the considered cases. This is an indication of the fact that going below the time granularity of 1 h does not lead to significant variations in results.

### C. Stored Energy Granularity

The last parameter that must be considered from the point of view of granularity is the energy storage. This means that we must define what is the quantum of energy to be considered within the battery. Since the quantization impacts the accounting of the amounts of consumed (and produced) energy during one time slot, and these amounts depend on the slot duration, we look at pairs of values  $(\Delta_T, Q_s)$ . Considering that the macro BS consumes between about 800 W (at peak traffic) and about 500 W (when no traffic is present), and that the PV panel production must be of the same order of magnitude (with somewhat higher peak, to compensate for periods of low or no production), with a time granularity of 1 h we look at stored energy granularity values equal to 100 Wh, 50 Wh, as well as 25 Wh. Assuming a peak hourly production from the PV panel around 2 kWh, this mean that the stored energy quantum is about 1/20, 1/40, 1/80 of the peak hourly energy production, about 1/8, 1/16, 1/32 of the maximum hourly energy consumption, and about 1/5, 1/10, 1/20 of the minimum hourly energy consumption. Results in Figure 14 show that for the hourly model the three quantization values produce very similar results of the average battery charge. When we go to a 30 minute time granularity, keeping the same stored energy quantum values means using 1/4, 1/8, 1/16 of the hourly energy consumption. With a 15 minute time granularity, keeping the same stored energy quantum values means using values that are 1/2, 1/4, 1/8 of the hourly energy consumption. Then, Figure 14 shows that values of the stored energy quantum of the order of 1/10 of the maximum hourly energy consumption can be a reasonable choice.

Figure 15 confirms this indication, since the values of average battery charge, of full and empty battery probability computed for  $\Delta_T = 1$  h, 30 and 15 minutes,  $Q_s = 100, 50$  and 25 Wh do not show significant differences, except for the case of very large PV panel, where the finer granularities allow a more accurate evaluation of the amount of energy that can be accepted in the battery.

### D. Takeaways

From our analysis we can draw the following conclusions. First of all, quantization has important effects on the model outputs. Developing models with a daily time granularity is not sufficient. A careful assessment of the system performance requires a time granularity that allows capturing the energy production and consumption variations during the day. If the model cannot carefully account for the fact that the energy that is produced when the battery is fully charged is lost and cannot be used, the predictions turn out to be optimistic. Our experiments indicate that a time granularity of 1 h can be a reasonable choice.

The impact of the day-type quantization is also relevant, specially if the histogram of the weather conditions produced with the equal-range approach turns out to have a triangular shape. In this case, an equal-probability quantization seems advisable. When an equal-probability quantization is used, 5 or 7 levels should be sufficient to capture the system performance with acceptable accuracy.

Finally, our results indicate that a quantization in the energy storage of the order of 1/10 of the maximum energy consumption per time slot is acceptable.

## V. EVALUATION OF THE BS POWER SYSTEM PERFORMANCE

In this section we evaluate, through numerical results derived from the model presented in Section III, the system performance, and we provide insight into its behavior. Our main goal in performing these experiments is three-fold: i) measure how different traffic profiles impact the amount of consumed/stored energy, so as to understand what can be the potential for the use of RES in different portions of the Radio Access Network (RAN), ii) discuss the impact, on the use of RES, of new generations of BSs, that are more parsimonious and more load proportional in energy consumption [2] with respect to current BSs [20], and iii) present the results that can be obtained in regions with irradiance patterns very different from what we considered so far (Turin and Paris); for this we look at the city of Maiduguri in Nigeria.

### A. Impact of traffic profiles

First, we analyse how the user traffic pattern impacts the dimensioning of the solar power system of the BS, in order to understand what can be the potential for the use of RES in different portions of the RAN.

1) *Turin*: Figure 13 shows the hourly average energy storage level for Turin. In night hours, the BS activity drains the energy stored in the battery during the peak production hours. At the end of the day, the balance can be positive (for good weather days, e.g., type 5), or negative (for bad weather days, e.g, type 1). We see that the differences between the curves for the residential and business traffic profiles are marginal. In addition, as expected, increasing PV panel sizes lead to larger amounts of stored energy in the battery. However, doubling the PV panel size (from 20 to 40 kW peak) has a large effect only for bad weather days, whose curve shows much higher energy values in the battery. For good weather days, the impact is minimal.

The main effect of the traffic profile is in the rate at which energy is drained from the battery during the evening (9:00 pm to midnight) and night (midnight to 5:00 am): the load from residential users is heavier on these time periods than that from business users, so that the battery level goes down faster for the residential traffic load.

To better visualize the differences between the two types of traffic profiles, Figure 16 shows the *maximum* values for the empty and full battery probabilities, respectively, versus the PV panel size. Each of these probabilities corresponds to the maximum value observed over all day hours, and over all day-types. We can see that the business area traffic is easier to handle, since it yields lower empty battery probability, and higher full battery probability for the same size of the PV panel. This is largely due to the higher correlation between the energy consumption induced by the business traffic profile and the energy generation of the PV panel. The fact that in a business area most of the traffic is generated during working

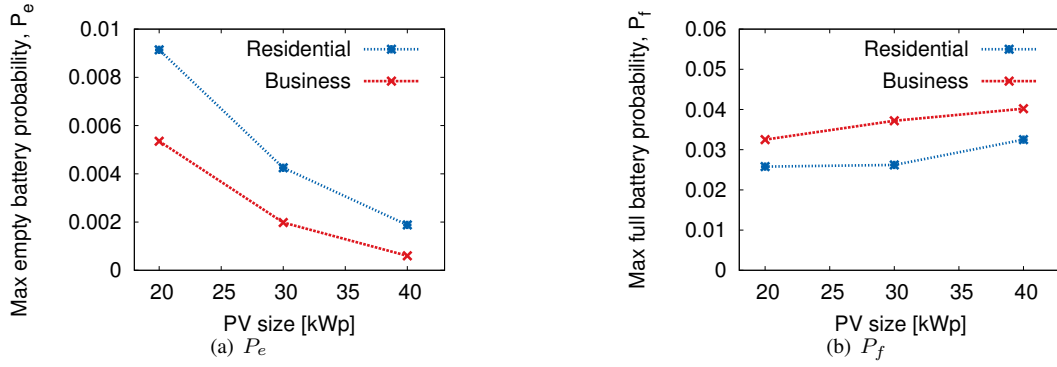


Fig. 16. Maximum hourly empty ( $P_e$ ) and full ( $P_f$ ) battery probabilities versus PV panel size, for Turin, with 5 day-types and equal-range discretization, time slot  $\Delta T = 1$ h, for  $C_B = 25$  kWh,  $Q_S = 100$  Wh, with residential and business weekday traffic profiles, adopting the Earth model.

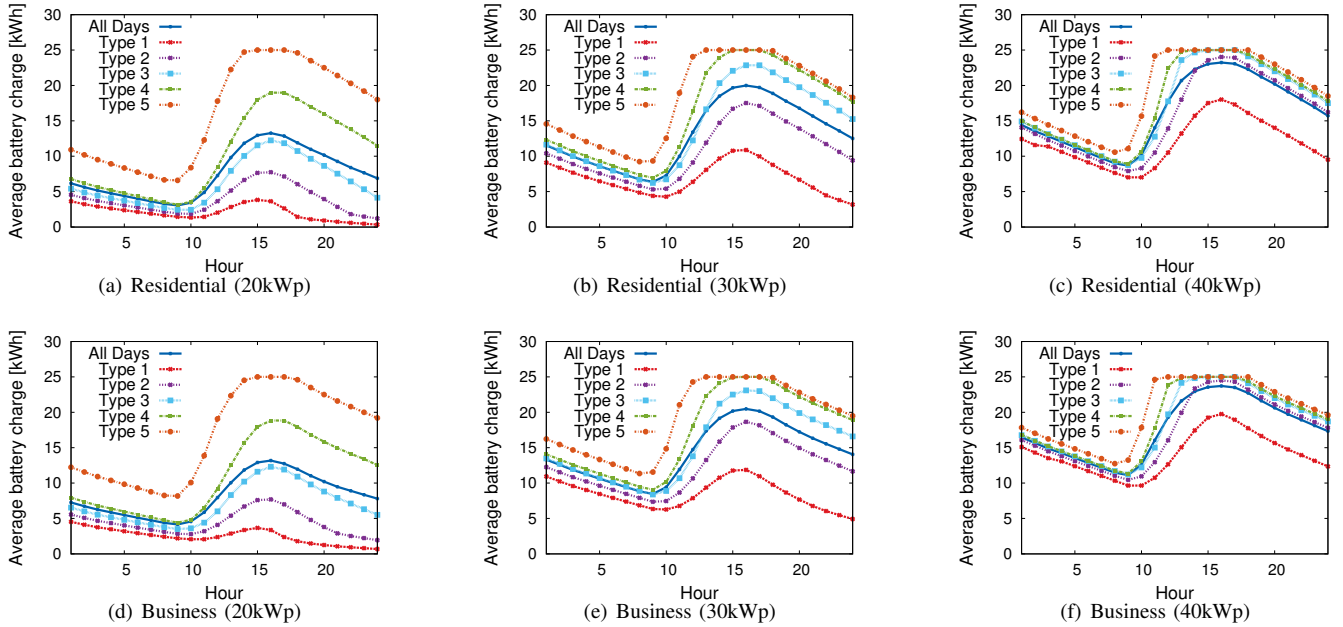


Fig. 17. Average hourly battery charge for a macro BS in Paris versus time, with  $N_W = 5$  and equal-probability discretization, time slot  $\Delta T = 1$ h, PV panel sizes 20, 30, and 40 kW peak,  $C_B = 25$  kWh, and  $Q_S = 100$  Wh, for both the residential and business weekday traffic profiles, adopting the Earth model.

3

hours allows the PV panel power to be immediately used to run the BS.

2) *Paris*: Figure 17 shows the hourly average energy storage level for Paris. The behavior of the curves is qualitatively similar to Turin, but the quantitative differences between different PV panel sizes are now much more pronounced.

To further visually compare the effect of different traffic profiles, in Figure 18 we plot the hourly average storage level for PV panel size equal to 30 kW peak, in residential and business areas, in Turin and Paris. Here we just show curves for days of types 1 and 5, and the average over all days. Once more, we see that differences are small, and this means that the solar option to power BSs is equally viable in business and residential areas.

## B. Impact of new generation base stations

The next aspect that we investigate is related to the technological evolution of BS technology, in particular as regards energy consumption. We evaluate the reduction of PV panel size that can be achieved with the BS technology transitioning from the one that led to the power model that we used so far and that we call EARTH model [20], to the one presented in [2], that we call the 2020 model. The latter type of BS exhibits an energy consumption pattern which is much lower, and also more proportional to the traffic load.

We derived results for the 2 x 2 macro BS model described in [2], which leads to a power saving of 47.7% at full load, when compared against [20]<sup>2</sup>.

<sup>2</sup>From [2], a BS with full load needs 702.6 W at full load and 114.5 W at zero load. From [20], instead, a BS with full load needs 1.344 kW at full load and 130 W at zero load.

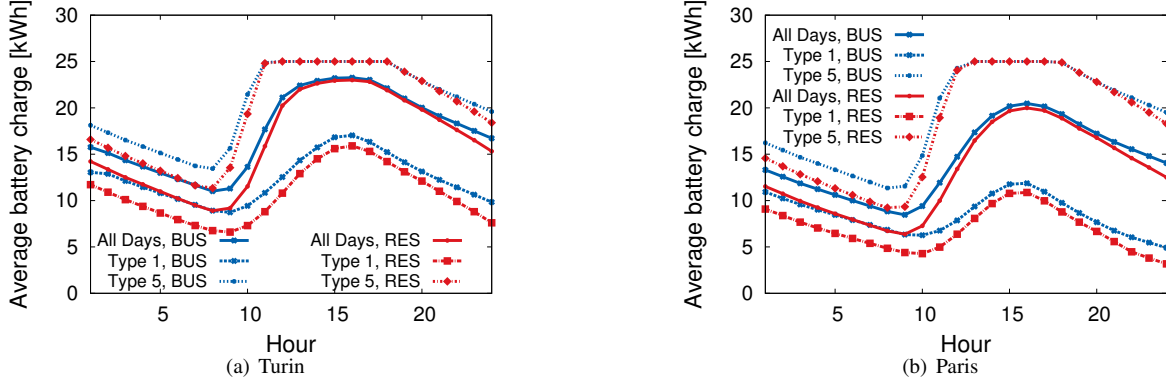


Fig. 18. Average hourly battery charge for a macro BS in Turin (equal-range discretization) and Paris (equal-probability discretization) versus time, with  $N_W = 5$  and time slot  $\Delta T = 1h$ , PV panel size 30 kW peak,  $C_B = 25$  kWh, and  $Q_S = 100$  Wh, for both the residential and business weekday traffic profiles, adopting the Earth model.

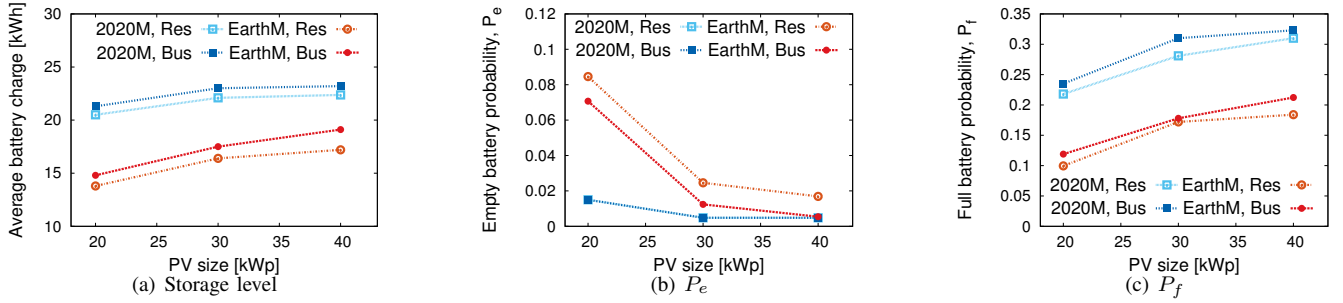


Fig. 19. Average battery charge level, empty ( $P_e$ ) and full ( $P_f$ ) battery probabilities versus PV panel size, for 2020 and Earth models (2020M and EarthM, respectively), in residential and business areas in the city of Turin.  $N_W = 5$  and equal-range discretization,  $\Delta T = 1h$ ,  $C_B = 25$  kWh, and  $Q_S = 100$  Wh.

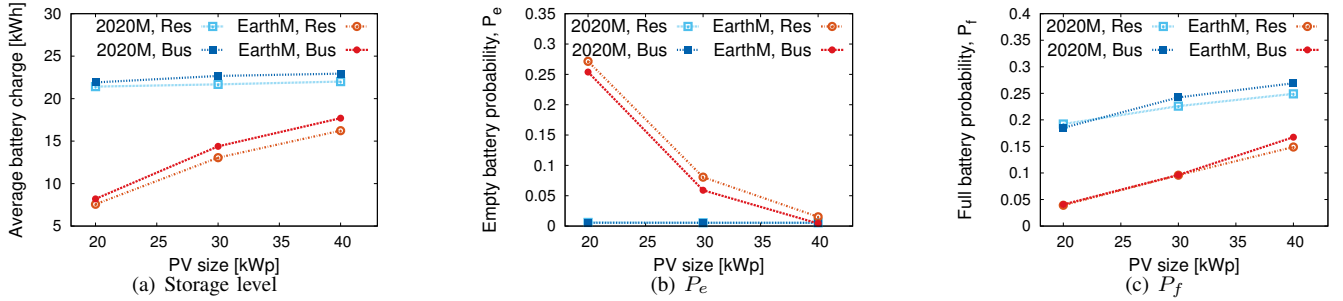


Fig. 20. Average battery charge level, empty ( $P_e$ ) and full ( $P_f$ ) battery probabilities versus PV panel size, for 2020 and Earth models (2020M and EarthM, respectively), in residential and business areas in the city of Paris.  $N_W = 5$  and equal-probability discretization,  $\Delta T = 1h$ ,  $C_B = 25$  kWh, and  $Q_S = 100$  Wh.

Figure 19 presents results for residential and business traffic profiles in Turin, while Figure 20 refers to Paris. By looking at the curves we see that the 2020 model yields better performance than the EARTH model, with half the panel size (20 kW peak instead of 40). For instance, the empty probability for a 20kWp panel size and 2020 model is 1/4 of the value of the EARTH model in Turin (19.b) and almost zero in Paris (20.b). Moreover, the battery remains full almost twice the time with the 2020 model, for all panel sizes. This means that the new generations of BSs are making the use of solar power less expensive, so that we can expect an increased diffusion of solar BSs in the coming years. The parallel technological

improvements in solar panels will further reinforce this trend.

### C. Impact of solar irradiance patterns

Finally, we look at the influence of geographic characteristics, which can have a big impact on solar irradiance patterns. Considering that, as we stated at the beginning of this paper, renewable energy sources can be particularly useful in areas where the power grid does not exist or is extremely unreliable, we look at the city of Maiduguri in Nigeria. Maiduguri is the capital of the Borno State in north-east Nigeria, and its population is around 1 million people. The city had severe energy problems over the last years, and is thus a very

TABLE II  
FULL AND EMPTY BATTERY PROBABILITY, MAIDUGURI, RESIDENTIAL  
PROFILE,  $C_B = 25$  kWh.

PV Size [kWp]	$P_f$	$P_e$
10	0.23	5.9e-02
20	0.36	5.6e-02
30	0.40	5.2e-02
40	0.40	5.0e-02

interesting candidate for the use of solar panels to power cellular communication equipment. The sub-saharan location of Maiduguri, at a latitude of about  $12^\circ$  north, guarantees a very high solar irradiance, somewhat diminished in the most rainy months, i.e., July, August and September. Considering, as usual, the least favorable period of the year for the analysis of the BS power system performance, we look at the solar irradiance in those three months. Even so, comparing the daily solar irradiance in Maiduguri to those of Turin and Paris, after a classification into 5 day-types, we see that in the least favorable day-type the maximum solar irradiance in Maiduguri is about four times higher than in both Turin and Paris, while the advantage of Maiduguri reduces to a factor 2 for the most favorable day-type.

Figure 21 shows the hourly battery charge for the case of residential area traffic, with battery capacity 25 kWh, and with PV sizes of 10, 20, 30, and 40 kW peak, respectively, in plots a), b), c) and d). We can note that the PV panel size significantly impacts only the curves for day-type 1 (the one with least irradiance). Otherwise, the curves are much more packed than in the cases of Turin and Paris, the only difference being in the speed at which the battery charge rises at the beginning of the day. The full and empty battery probabilities are reported in Table II for different PV panel sizes. In this case we see that outage probability differences are very small, in spite of large PV panel size variations. This result tells us that the system bottleneck is more in the battery capacity rather than in the energy production capacity.

For this reason, Figure 22 shows the hourly average battery charge with PV size 10 kW peak, and with battery capacity equal to 25, 35, and 50 kWh, respectively, in plots a), b), and c). We can note that the average battery charge grows significantly for all day-types for increasing battery capacity, thanks to the excess energy production in days of high solar irradiance which is not wasted with batteries of adequate size. The empty battery probability remains close to 5% for all battery capacities, mainly due to longer sequences of rainy days.

The observation of the Maiduguri results, and their comparison against those of Paris and Turin, tell us that optimal BS power solutions based on PV panels and batteries can be extremely different from one geographical location to another. In Maiduguri a small PV panel is sufficient, but a larger battery is necessary to obtain very small outage probabilities. Turin and Paris require much larger PV panels, but can live with smaller batteries, since the outage probability is more driven by the PV panel size than by the battery capacity. In order to be able to observe these effects, carefully engineered stochastic

models are necessary, and this is the issue we address in this paper.

## VI. CONCLUSIONS

This paper focused on the analysis of the effects of quantization in the analytical models that are used to dimension the power system of solar-powered off-grid base stations. Quantization was investigated for the three main model parameters: time, weather (in terms of solar irradiance), and energy storage. That is, we discussed the size of the time slot according to which the discrete-time model evolves, the number of levels that are used to describe solar irradiance, and the quantum of energy that is considered when looking at the system batteries. Our study unveiled the critical role of quantization for a correct power system dimensioning. Our main findings can be summarized by saying that a credible and accurate model requires: i) a time granularity that allows capturing the energy production and consumption fluctuations *during* the day, and our experiments indicate that a time slot equal to 1 h can be a reasonable choice; ii) the discretization of the weather conditions according to 5 or 7 levels of average daily solar irradiance; iii) a storage energy quantum of the order of 1/5 of the minimum energy consumption per time slot.

In addition, we presented numerical results showing the impact of different traffic profiles on the amount of consumed/stored energy. The differences between the curves for residential and business traffic profiles are marginal for both cases of Turin and Paris. Moreover, we discussed the impact on the use of renewable energy sources of the technological evolution of base stations, with new product generations that are more parsimonious and more load proportional in energy consumption. Our analysis showed that it is possible to achieve a better performance, with half the solar panel size, with the coming generations of base station technology. Finally, we considered the case of Maiduguri in Nigeria, where solar irradiation is much higher than for both Paris and Turin, showing that in this case small solar panels are sufficient, but larger batteries are necessary in order to reduce outage probabilities to around 5% during the rainy season.

Our work helps understanding how the correct design of solar power systems for off-grid base stations should be approached. In addition, it shows that the solar option is becoming extremely attractive to power new generations of base stations. If the promised improvements in solar cell technologies will materialize soon, bringing efficiency from the current 20 % to about 50 %, in the coming years, the solar option will become the default solution to power base stations in many geographical areas.

## ACKNOWLEDGMENTS

This research is partially funded by the first author's individual grants from CNPq (Brazil), and by the Politecnico di Torino Visiting Professors 2015/2016 Grant (Italy).



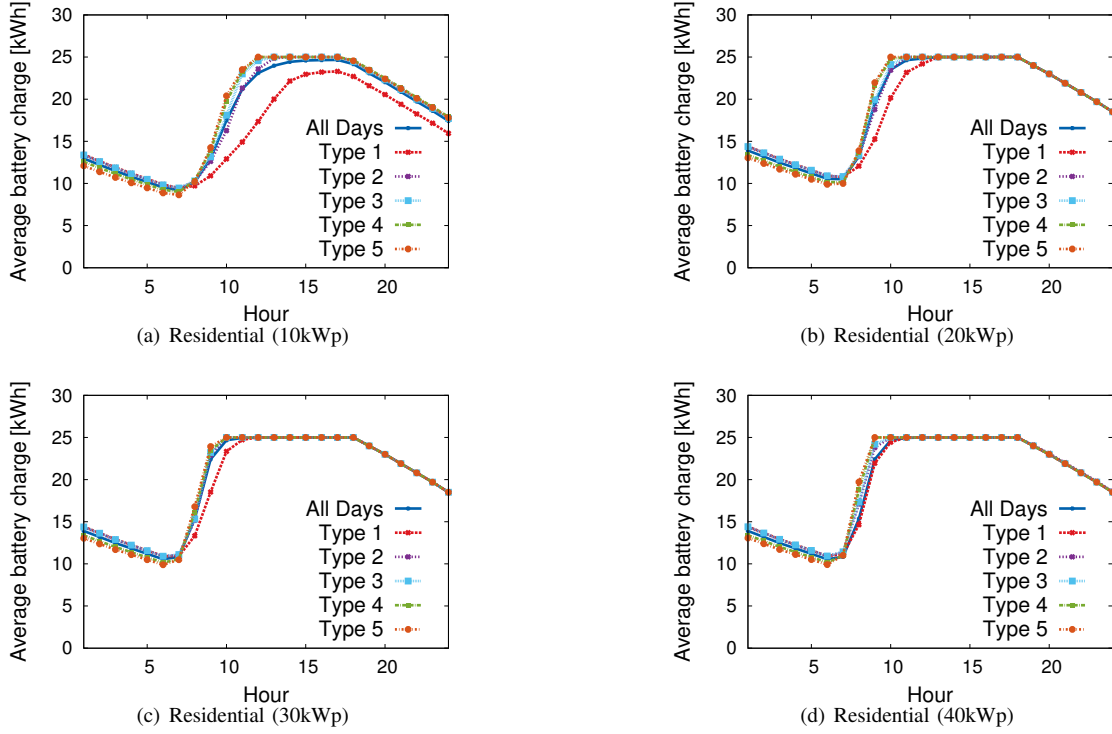


Fig. 21. Average hourly battery charge for a macro BS in Maiduguri versus time, with  $N_W = 5$  and equal-probability discretization, time slot  $\Delta T = 1h$ , PV panel sizes 10, 20, 30, and 40 kW peak,  $C_B = 25$  kWh, and  $Q_S = 100$ Wh (50Wh in case of PV panel size 10 kW peak), for the residential weekday traffic profiles, adopting the EARTH model.

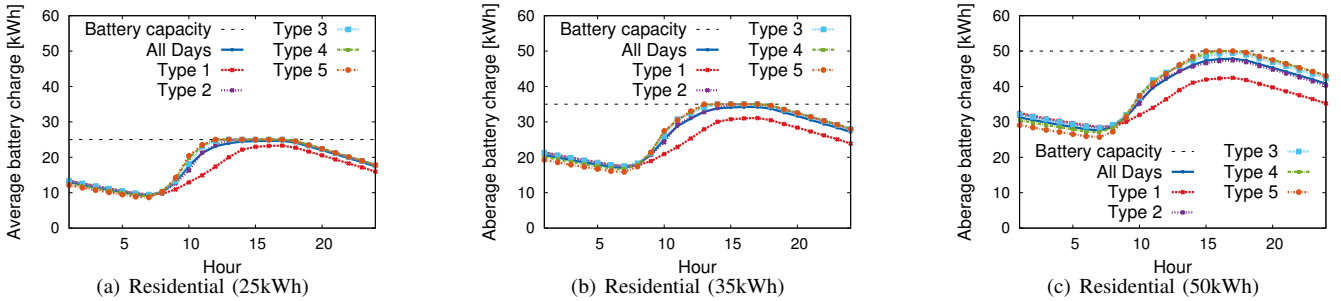


Fig. 22. Average hourly battery charge for a macro BS in Maiduguri versus time, with  $N_W = 5$  and equal-probability discretization, time slot  $\Delta T = 1h$ , PV panel size 10 kW peak, battery capacities 25, 35, 50 kWh, and  $Q_S = 100$  Wh, for the residential traffic profiles.

## REFERENCES

- [1] M. Di Renzo, *Energy-Efficiency Metrics and Performance Trade-Offs of GREEN Wireless Networks*. John Wiley & Sons, Ltd, 2015, pp. 43–54. [Online]. Available: <http://dx.doi.org/10.1002/9781118759257.ch3>
- [2] B. Debaillie, C. Desset, and F. Louagie, “A flexible and future-proof power model for cellular base stations,” in *IEEE 81st Vehicular Technology Conference, VTC Spring 2015, Glasgow, United Kingdom, 11-14 May, 2015*, 2015, pp. 1–7. [Online]. Available: <https://doi.org/10.1109/VTCSpring.2015.7145603>
- [3] L. Budzisz, F. Ganji, G. Rizzo, M. A. Marsan, M. Meo, Y. Zhang, G. Koutitas, L. Tassiulas, S. Lambert, B. Lannoo, M. Pickavet, A. Conte, I. Haratcherev, and A. Wolisz, “Dynamic resource provisioning for energy efficiency in wireless access networks: a survey and an outlook,” *IEEE COMMUNICATIONS SURVEYS AND TUTORIALS*, vol. 16, no. 4, pp. 2259–2285, 2014.
- [4] H. A. H. Hassan, L. Nuaymi, and A. Pelov, “Renewable energy in cellular networks: A survey,” in *IEEE Online Conference on Green Communications, OnlineGreenComm 2013, October 29-31, 2013*, 2013, pp. 1–7. [Online]. Available: <https://doi.org/10.1109/OnlineGreenComm.2013.6731020>
- [5] GSMA Intelligence, “The Mobile Economy - Africa 2016,” Mobile Economy, Tech. Rep., 2016.
- [6] V. Chamola and B. Sikdar, “Solar powered cellular base stations: current scenario, issues and proposed solutions,” *IEEE Communications Magazine*, vol. 54, no. 5, pp. 108–114, 2016. [Online]. Available: <http://dx.doi.org/10.1109/MCOM.2016.7470944>
- [7] K. Samdanis, P. Rost, A. Maeder, M. Meo, and C. Verikoukis, “Green Communications: Principles, Concepts and Practice,” 2015. [Online]. Available: <http://porto.polito.it/2649998/>
- [8] W. Van Heddeghem, S. Lambert, B. Lannoo, D. Colle, M. Pickavet, and P. Demeester, “Trends in Worldwide ICT Electricity Consumption from 2007 to 2012,” *Comput. Commun.*, vol. 50, pp. 64–76, Sep. 2014.
- [9] M. A. Marsan, G. Bucalo, A. D. Caro, M. Meo, and Y. Zhang, “Towards zero grid electricity networking: Powering bss with renewable energy sources,” in *IEEE International Conference on Communications, ICC 2013, Budapest, Hungary, June 9-13, 2013, Workshops Proceedings*, 2013, pp. 596–601. [Online]. Available: <http://dx.doi.org/10.1109/ICCW.2013.6649303>
- [10] V. Chamola and B. Sikdar, “Dimensioning stand-alone cellular base station using series-of-worst-months meteorological data,” in *ICCS*. IEEE, 2014, pp. 339–343.

- [11] —, “Resource provisioning and dimensioning for solar powered cellular base stations,” in *GLOBECOM*. IEEE, 2014, pp. 2498–2503.
- [12] M. Meo, Y. Zhang, R. Gerboni, and M. A. Marsan, “Dimensioning the power supply of a LTE macro BS connected to a PV panel and the power grid,” in *2015 IEEE International Conference on Communications, ICC 2015, London, United Kingdom, June 8-12, 2015*, 2015, pp. 178–184. [Online]. Available: <http://dx.doi.org/10.1109/ICC.2015.7248318>
- [13] V. Chamola and B. Sikdar, “Outage estimation for solar powered cellular base stations,” in *ICC*. IEEE, 2015, pp. 172–177.
- [14] M. H. Alsharif, J. Kim, and J. H. Kim, “Green and sustainable cellular base stations: An overview and future research directions,” *Energies*, vol. 10, no. 5, 2017.
- [15] K. Kusakana and H. J. Vermaak, “Hybrid renewable power systems for mobile telephony base stations in developing countries,” *Renewable Energy*, vol. 51, no. C, pp. 419–425, 2013.
- [16] A. M. Aris and B. Shabani, “Sustainable power supply solutions for off-grid base stations,” *Energies*, vol. 8, no. 10, pp. 10904–10941, 2015.
- [17] S. Vikas Khare and P. Baredar, “Status of solar wind renewable energy in india,” *Renewable and Sustainable Energy Reviews*, vol. 27, pp. 1–10, 2013.
- [18] J. Song, V. Krishnamurthy, A. Kwasinski, and R. Sharma, “Development of a markov-chain-based energy storage model for power supply availability assessment of photovoltaic generation plants,” *IEEE Transactions on Sustainable Energy*, vol. 4, no. 2, pp. 491–500, April 2013.
- [19] G. Leonardi, M. Meo, and M. A. Marsan, “Markovian models of solar power supply for a LTE macro BS,” in *2016 IEEE International Conference on Communications, ICC 2016, Kuala Lumpur, Malaysia, May 22-27, 2016*, 2016, pp. 1–7. [Online]. Available: <http://dx.doi.org/10.1109/ICC.2016.7510698>
- [20] EARTH (Energy Aware Radio and network technologies) project, “Energy efficiency analysis of the reference systems, areas of improvements and target breakdown,” 2012.
- [21] Y. Zhang, L. Budzisz, M. Meo, A. Conte, I. Haratcherev, G. Koutitas, L. Tassiulas, M. A. Marsan, and S. Lambert, “An overview of energy-efficient base station management techniques,” in *Proc. of TIWDC’13 (24th Tyrrhenian Int. Workshop on Digital Communications)*, September 2013, ConferenceProceedings.
- [22] G. Auer, V. Giannini, C. Desset, I. Gódor, P. Skillermarck, M. Olsson, M. A. Imran, D. Sabella, M. J. Gonzalez, O. Blume, and A. J. Fehske, “How much energy is needed to run a wireless network?” *IEEE Wireless Commun.*, vol. 18, no. 5, pp. 40–49, 2011. [Online]. Available: <http://dblp.uni-trier.de/db/journals/wc/wc18.html#AuerGDGSOISGBF11>



**Ana Paula Couto da Silva** earned her Ph.D. degree in Computer and System Engineering from the Federal University of Rio de Janeiro (2006). She was with IRISA-Rennes in 2005 and 2007, and with Politecnico di Torino in 2008, 2010, 2011 and 2016 (as visiting professor). She is with the Computer Science Department at the Federal University of Minas Gerais since 2013 as associate professor. Her areas of interest are in the field of modelling and analysis of computer systems and energy efficient networking, characterization of Internet Traffic and

complex network theory.



**Daniela Renga** is a Ph.D. student in Electrical, Electronics and Communications Engineering at the Politecnico di Torino, Italy. She received the Master degree in Computer and Communication Networks Engineering in 2014 from the Politecnico di Torino. In 2004 she received a Laurea degree in Medicine from the Università degli Studi di Torino, Italy. Her research interests are in the fields of energy efficient wireless networks, resource management, network modeling, smart grids and renewable energy sources for sustainable mobile networks.



**Michela Meo** received the Laurea degree in Electronic Engineering in 1993, and the Ph.D. degree in Electronic and Telecommunications Engineering in 1997, both from the Politecnico di Torino, Italy. Since November 2006, she is professor at the Politecnico di Torino. She co-authored about 200 papers and edited a book with Wiley and special issues of international journals, including *ACM Monet*, *Performance Evaluation*, and *Computer Networks*. She chairs the Steering Committee of IEEE Online-GreenComm and the International Advisory Council of ITC. She is associate editor of *IEEE Communications Surveys & Tutorials*, area editor of *IEEE Transactions on Green Communications and Networking*, and was associate editor of *IEEE Transactions of Networking*. She was program co-chair of several conferences among which *ACM MSWiM*, *IEEE Online GreenComm*, *IEEE ISCC*, *IEEE Infocom Miniconference*, *ITC*. Her research interests include performance evaluation and modeling, green networking and traffic classification and characterization.



**Marco Ajmone Marsan** is Full Professor at the Politecnico di Torino and part time Research Professor at the IMDEA Networks Institute in Spain. He was Vice-Rector for Research, Innovation and Technology Transfer of the Politecnico di Torino and the Director of the Istituto di Elettronica e Ingegneria dell'Informazione e delle Telecomunicazioni of the Italian National Research Council (CNR). In the same period, he was also coordinating the activities of the ICT Department of CNR. He was the President of the Italian Association of Telecommunication

Professors and the Italian Delegate at the ICT Committee and at the IDEAS Committee of the 7th Framework Programme (FP7) of the European Commission. He was awarded a honorary degree in Telecommunication Networks from the Budapest University of Technology and Economics. He was named Commendatore dell'Ordine al Merito della Repubblica Italiana by the President of Italy. He is a Life Fellow of the IEEE, and a member of the Accademia Europaea and of the Academy of Sciences of Torino. He is among the “ISI highly cited researchers” in Computer Science. Marco Ajmone Marsan was a member of the editorial board of the journal “ACM/IEEE Transactions on Networking”, for which he also chaired the Steering Committee. He is a member of the editorial board of the journals “Computer Networks” and “Performance Evaluation” of Elsevier, and of the ACM Transactions on Modeling and Performance Evaluation of Computer Systems. He was general chair of INFOCOM 2013.